Pergamon

Journal of Structural Geology, Vol. 17, No. 3, pp. 345 to 356, 1995

0191-8141/95 $9.50+0.00

0191-8141(94)00065-4

Reorientation mechanisms of phyllosilicates in the mudstone-to-slate transition at Lehigh Gap, Pennsylvania

NEI-CHE HO, DONALD R. PEACOR and BEN A. VAN DER PLUIJM

Department of Geological Sciences, University of Michigan, Ann Arbor, MI 48109, U.S.A.

(*Received* 29 *November* 1993; *accepted in revised form* 2 *May* 1994)

Abstract—The mudstone-to-slate transition of the Martinsburg Formation at Lehigh Gap, Pennsylvania, was re-examined using a new transmission-mode X-ray texture goniometer, supplemented by SEM, XRD, and optical studies. Three mesoscopic zones are recognized in the outcrop: (I) mudstone, (II) transition, and (III) slate zone. In the mudstone zone, the mica basal planes are parallel to bedding whereas the preferred orientation of the chlorite basal planes is up to 30° shallower than bedding. The angular difference between chlorite and mica decreases towards the transition zone, becoming subparallel at *ca.* 50 m from the contact with the overlying Shawangunk Formation. In the transition zone, the preferred orientations of both mica and chlorite are intermediate to bedding and cleavage orientations, which is consistent with mechanical reorientation of phyllosilicates. This is supported by a decrease in March strain with a minimum at *ca.* 95 m from the contact for both mica and chlorite. SEM observations similarly show the importance of grain rotation in large detrital grains. In the slate zone, both chlorite and mica orientations are parallel to cleavage. Chlorite and mica in the cleavage orientation of the slate zone have high Fe contents, whereas low-Fe mica and Mg > Fe chlorite dominate in the mudstone and transition zone, which indicates that dissolution-neocrystallization is the dominant mechanism in the slate zone. Thus, mechanical rotation of large detrital grains is important in the early stages of cleavage development, with dissolution–neocrystallization occurring at all stages and becoming dominant in the more evolved stages.

INTRODUCTION

Slaty cleavage development has been a much-debated process for nearly 150 years (e.g. Sorby 1853, Williams 1972, Wood 1974, White & Knipe 1978, Engelder & Marshak 1985). The two principal mechanisms that have been proposed for reorientation of phyllosilicates associated with cleavage formation are: (1) mechanical rotation of pre-existing grains, as implied, for example, by detrital phyllosilicate grains that are oriented parallel to bedding in the absence of foliation and parallel to foliation elsewhere, and (2) dissolution and neocrystallization ('pressure solution'). During cleavage formation, phyllosilicate grains aligned with (001) approximately parallel to the maximum shortening direction, Z, become preferentially strained (e.g. Hobbs *et al.* 1976, van der Pluijm & Kaars-Sijpesteijn 1984). Dissolution with subsequent neocrystallization will preferentially affect deformed grains because they have high internal strain energy (Wintsch 1985). Thus, the proportion of phyllosilicate grains inclined to the XY plane at large angles decreases. New grains may crystallize with (001) planes parallel to the developing foliation under the influence of stress (Kamb 1959), or parallel to the planar surface of pre-existing grains (Oertel 1970).

Mechanical rotation and dissolution/neocrystallization are end-member processes that may be active during cleavage formation. Geological parameters such as temperature, fluid/rock ratio, the composition of pore fluids, porosity, state of lithification, and the strain rate may determine which mechanism is dominant. For example, at low temperatures or high strain rates, rotation of inequant grains may be dominant relative to dissolution and neocrystallization, whereas at high temperatures and high fluid/rock ratios dissolution may occur so rapidly as to destroy evidence of grain deformation (Lee *et al.* 1986).

The exposure of the Martinsburg Formation at Lehigh Gap, Pennsylvania (Fig. 1) has long served as a locality

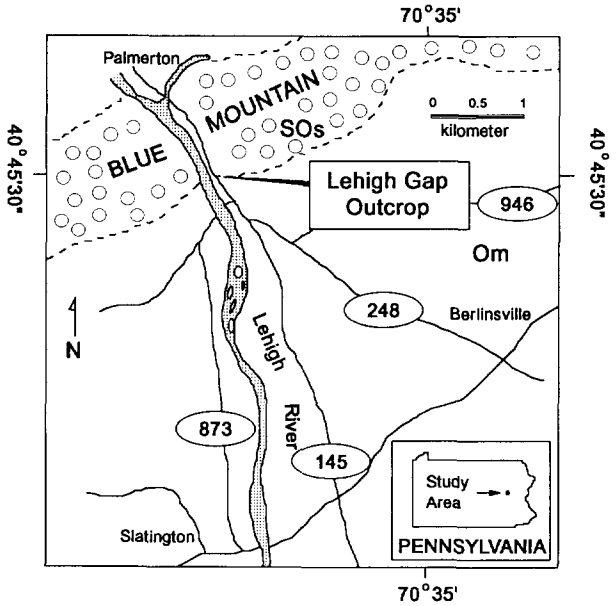

Fig. 1. Geological map and location of the Lehigh Gap outcrop in Pennsylvania. Om—Ordovician Martinsburg Formation. SOs—Silurian Shawangunk Formation.

for detailed study of cleavage formation. Well-defined slaty cleavage is regionally developed throughout the Martinsburg Formation except at Lehigh Gap, where there is gradual and continuous development of slaty cleavage over a distance of only 100 m. Mudstone is preserved at the contact with the overlying Shawangunk Formation, presumably because that competent formation created a local strain shadow (Epstein & Epstein 1969), and the mudstone-to-slate transition can be clearly traced, with slaty cleavage appearing approximately 60 m from the contact. Furthermore, bedding uniformly dips ≈45° to the north, with cleavage oriented approximately perpendicular to bedding, thus affording a sharp contrast in orientations of these structural elements.

Maxwell (1962) hypothesized that the cleavage in the Martinsburg slate is the result of deformation of unconsolidated sediments, with mechanical reorientation during fluid escape as the principal mechanism of cleavage formation. Carson (1968) and Alterman (1973) further supported this hypothesis, but it was questioned by others (e.g. Epstein & Epstein 1969, Boulter 1974, Holeywell & Tullis 1975). Holeywell & Tullis (1975) utilized an early X-ray pole figure device to measure preferred orientations of mica and chlorite across the transition. Their observations included: (1) chlorite has a preferred orientation that has a rake ≈20° less steep than that of bedding and of the preferred orientation of mica, except where chlorite is parallel to the regional cleavage; (2) the orientation of mica gradually changes towards that of cleavage in advance of chlorite, the chlorite orientation being unchanged 30 m further along the outcrop. Based on these results, a mechanical rotation mechanism was ruled out and 'pressure solution' was proposed to be the dominant mechanism. This interpretation was generally supported by other workers employing chemical data (Wintsch 1978, Woodland 1982, Wintsch *et al.* 1991), optical studies (Beutner 1978, Woodland 1982) and transmission electron microscopy (TEM) (Lee *et al.* 1986).

Nevertheless, the data supporting only dissolution and neocrystallization are incomplete. For example, the critical X-ray texture data were obtained only from 'great-circle scans' (see Holeywell & Tullis 1975 for details), rather than from complete pole figures. Secondly, phyllosilicates in the fine-grained matrix may behave differently than detrital grains as shown, for example, in a recent study of Welsh slates (Li *et al.* 1994). Detrital phyllosilicate grains were observed to occur primarily as chlorite–mica stacks, were oriented parallel or subparallel to bedding, and were commonly markedly deformed. In contrast, matrix phyllosilicates consisted predominantly of authigenic white mica and chlorite (not as stacks), with (001) planes oriented parallel to either bedding or cleavage. Few grains were observed to have orientations intermediate to bedding and cleavage, similar to the observations for the mudstone-to-slate transition at Lehigh Gap (Lee *et al.* 1986). The TEM observations of Lee *et al.* (1986) were only obtained for fine-grained matrix phyllosilicates, with no observations of coarse detrital grains. We have therefore used an automated pole figure device (van der Pluijm *et al.* 1994), complemented by scanning electron microscope (SEM) observations, to resolve questions about the relative contributions of mechanical rotation and dissolution/neocrystallization to cleavage formation at Lehigh Gap and to discriminate between the roles of detrital and authigenic grains.

GEOLOGICAL SETTING AND SAMPLE COLLECTION

The Martinsburg Formation (Keith 1894) forms a continuous but poorly exposed belt of outcrops along the Appalachian Valley (Fig. 1). It was deposited as a sequence of greywackes and mudstones, characterized by well-developed shelf, slope, and basin facies. The Martinsburg Formation, together with the underlying Jacksonburg Limestone, recorded the Middle Ordovician transition of the North American continent from a tectonically passive carbonate shelf to an active plate margin (Lash 1987, Stephens & Wright 1981). By the end of Late Ordovician time, the Martinsburg basin was filled with shallow-water-subaerial clastic sediment of the overlying Shawangunk Formation. Cleavage developed regionally during the late Paleozoic (Wintsch & Kunk 1992, Housen *et al.* 1993).

Samples for this study were originally collected for magnetic fabric study (Housen & van der Pluijm 1991, Housen *et al.* 1993). From this collection, 13 samples separated by 2–20 m were chosen (Table 1 and Fig. 2). Semi-quantitative analyses of proportions of major constituent minerals using integrated intensities from powder X-ray diffractometer (XRD) patterns resulted in the following approximate weight percents: quartz, 45%; illite, 35%; chlorite, 10%; plagioclase, 10% (Lee *et al.* 1986). The relative proportions of these four dominant minerals are similar for all samples ranging through the mudstone-to-slate transition.

METHODS OF STUDY

X-ray pole figure device

The crystallographic preferred orientation measurements presented in this paper were performed on a modified X-ray pole figure device attached to an Enraf-Nonius CAD4 single-crystal diffractometer equipped with a Mo source. The device was designed and constructed to measure preferred orientation of phyllosilicates in the transmission mode (Schulz 1949), which provides data over a much larger range of orientations than the reflection mode (e.g. Wenk 1985). The volume of sample analyzed is about 1 mm^2 × 0.2 mm (area × thickness). Output from this system is a contoured pole figure plot, with intensity normalized and expressed in

Table 1. Bedding/cleavage and preferred orientation data of samples

Sample	Reference	Distance	Bedding	Cleavage	Mica 1	Mica 2	Chl[1]	Chl[2]
1	10H	6	261/45N		261/45N		266/15N	
2	19AD	34	261/42N		261/42N		257/24N	
3	19BB	37	267/44N		264/46N		257/40N	
4	22AB	50	266/56N		—		—	
5	22BA	53	286/52N		282/45N		272/40N	
6	23A	74	265/50N	126/48S	230/48N		232/38N	
7	24A	77	259/54N	113/78S	258/28N	113/78S	240/36N	119/78S
8	25AC	85	266/53N	114/62S	246/28N		223/22N	
9	25BC	87	262/53N	116/47S	276/72N		252/12N	
10	26AB	91	266/47N	119/54S	286/12N		260/2S	
11	27A	98	260/38N	107/72S		107/62S		100/60S
12	28D	104	261/42N	113/74S	250/40N	107/70S	246/34N	102/68S
13	31BC	128	264/39N	96/72S		104/68S		92/78S

[1]Reference: for comparison with magnetic fabric data (Housen & van der Pluijm 1991).
[2]Orientation of fabric element is given as strike/dip.

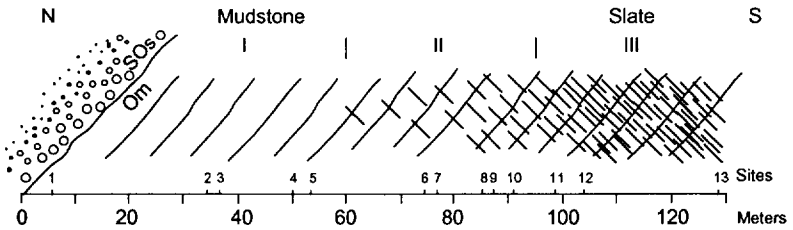

Fig. 2. Schematic diagram of the Lehigh Gap outcrop, showing the bedding and cleavage attitudes and stages of cleavage development. Locations of sample stations and horizontal distance in meters from the Martinsburg–Shawangunk contact are marked at the bottom. Three mesoscopic zones are defined in the outcrops: mudstone (I), transition (II) and slate (III) zones.

multiples of random distribution (m.r.d.). The system and procedure have been described by van der Pluijm *et al.* (1994) and Ho (unpublished M.S. thesis).

The goniometer performs two kinds of motion. It rotates the sample about the axis perpendicular to the sample surface (herein called χ rotation), and about the axis that defines the angle 2θ (herein called ω rotation), as shown in Wenk (1985). The scan range is sampled in steps, and covers a range with 144 increments, each of 2.5° of the χ rotation (changing azimuth angle), and nine increments of 5° for the ω rotation (changing pole distance). This type of scan covers approximately three fourths of angular space, and is distinct from the 'great-circle scan' used by Holeywell & Tullis (1975), where data are obtained only for one great circle normal to the sample surface. Time of measurement at each sample point can be varied, but results from the same sample but for different times show that times as short as 2 s effectively give the same result as those for 10 s, with only a small reduction in precision (Ho, unpublished M.S. thesis). The 10-Å peak was used as a measure of mica (001) orientation, and the 7-Å peak for chlorite (002) was used, in part because kaolinite, which when present gives a peak at the same position, is absent or present in negligible amounts (Lee *et al.* 1986). We note that texture goniometry is generally able to resolve multiple maxima within a sample, rather than average their orientations, as is the case in, for example, magnetic fabric analysis.

Sample preparation

Two sections, one for X-ray measurements and one for SEM observations, were prepared from each sample. A section about 200 μm in thickness, cut perpendicular to both bedding and cleavage, was first obtained. The thickness of this section was measured in order to calculate X-ray absorption factors. A polished thin section was subsequently prepared for SEM observations with surface oriented parallel to that of the first section.

MARCH MODEL

The March model (March 1932) is a mathematical model that predicts changes in preferred orientations, and has been used as a measure of strain in natural rocks (e.g. Tullis & Wood 1975, Oertel 1983, Chen & Oertel 1989, Chen & Oertel 1991). The March model is concerned with the geometrical consequences of homogeneous strain that uniformly affects all components of a given material. Grains with measurable orientations only play a role of passive markers and are taken to be otherwise mechanically indistinguishable from the rock in which they are embedded. The orientation of markers is measured by pole figure analysis and the changes in orientation can be reflected in the changes in the pole figure. March (1932) derived a formula relating the final

pole densities in the principal directions of the strain to an original uniform density. The relationship is: $e_i = \rho_i^{-1/3}$, where e_i is a principal strain, expressed as the change of length divided by the original length, and ρ_i is a principal pole density, normalized by dividing it by the average pole density for all orientations. The principal strain refers to the total strain that a homogeneous rock has undergone if it formed without preferred orientation of its constituent grains, or to the relative strain if there was a preferred orientation in the original rock and that original fabric can be characterized.

Mechanical rotation of grains, however, is not the only process contributing to cleavage formation, and it is therefore not clear that the March model can represent the actual strain state if other mechanisms are active, and also not clear whether all other assumptions of the model are valid. Etheridge & Oertel (1979) further pointed out that it is important to distinguish results referring to tectonic strain from those that measure the total strain, where the latter includes any pre-tectonic deformation. In spite of these limitations, the March model does provide a quantitative measure of the relative geometry and intensity of the orientation distribution (the shape of the preferred orientation ellipsoid). In this paper we therefore use the March model as an analytical tool to make comparisons of the differences in degree of preferred orientation between samples on a quantitative basis. The values derived from the March model will be referred to as 'March strains' in this paper to distinguish them from tectonic or total strain.

RESULTS

Crystallographic preferred orientation

Intensity data were obtained for 13 samples using a pole-figure device, and corrected for background, irradiated volume, and absorption effects (van der Pluijm *et al.* 1994). Contoured intensity data were plotted as equal-area projections in the specimen co-ordinate system. For most samples, two sets of data from different areas were obtained for comparison. There is little difference in both orientation and intensity for such sets of samples with well-defined maxima (e.g. sample 1). The differences are up to 10° in orientation and 8% in intensity for samples with ill-defined maxima (e.g. sample 9). Figure 3 shows results for representative data sets for all samples. Given the orientations of the samples, the preferred orientations of mica and chlorite for each sample in the geographical co-ordinate system were reconstructed. These data are included in Table 1. Lower-hemisphere equal-area projections for the preferred orientations of the mica (001) and chlorite (002) reflections of all samples in geographical co-ordinates are shown in Figs. 4(a) & (b). For reference, the bedding and cleavage orientations along the outcrop are also given (Fig. 4c). The outcrop is subdivided into three zones based on field observations of cleavage. These mesoscopic zones are: (I) mudstone zone, (II) transition zone, and (III) slate zone.

Mica (001) planes are preferentially oriented subparallel to bedding up to sample 3 (mudstone zone), but shift away from bedding in progressive samples in the transition zone. For sample 7, in the transition zone, two preferred orientations were found, a weaker one in the bedding orientation, and a stronger one parallel to the cleavage orientation. The measured preferred orientation of mica shifts slightly further toward the cleavage orientation in samples 8 and 9, with a large shift to the cleavage orientation occurring for sample 11. In all samples from the slate zone (samples 11–13), there is a mica preferred orientation parallel to the cleavage. There is a second, weaker preferred orientation in the bedding orientation only for sample 12.

The preferred orientations of chlorite in those samples that do not have a mesoscopic cleavage define a path that is slightly different from that of mica. Closest to the contact with the Shawangunk Formation, the preferred orientation of chlorite is approximately 30° shallower than bedding. It approaches the mica orientation in sample 3, and the two orientations remain subparallel further along the outcrop, i.e. chlorite shifts increasingly away from bedding, toward the cleavage orientation. Two preferred orientations of equal intensity were observed for sample 7, parallel to bedding and cleavage, respectively. A large shift occurs between sample 10 and sample 11. All the samples in the slate zone (samples 11–13) have chlorite preferred orientation parallel to cleavage. Sample 12 also has a weak chlorite preferred orientation in the bedding orientation.

March strains

March strains are shown in Fig. 5, which is a plot of the value of e_3, as listed in Table 3. Maximum March strains of mica occur in samples 2 and 13, and are a minimum in sample 11. Between samples 2 and 11, there is a trend of generally decreasing March strains, whereas they increase beyond sample 11.

The values for chlorite show a similar trend, but are less well-defined in the transition zone. The March strains reach a maximum at sample 2, a minimum at sample 10, and vary irregularly between these two points. Large strains occur in samples 6 and 8, and a small strain in sample 7. However, because of the presence of two equally intense preferred orientations in sample 7, this March strain is not meaningful. Therefore, a dashed line is drawn, connecting samples 6 and 8. As for mica, the March strains for chlorite increase beyond sample 10.

SEM observations

All SEM images were obtained in back-scattered electron (BSE) mode. The images shown in Fig. 6 are oriented so that the bedding and cleavage directions are the same in each image. Moreover, the images

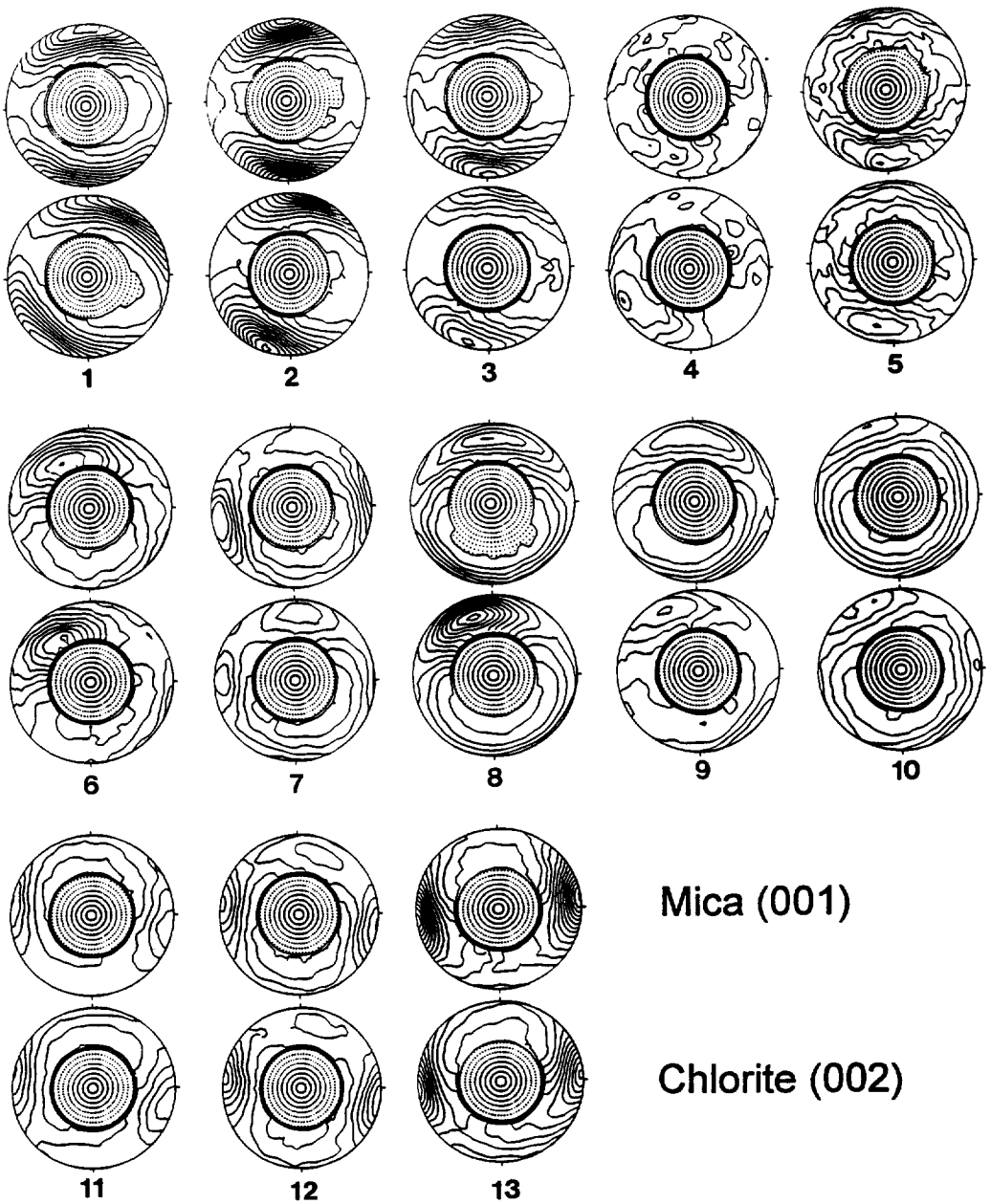

Fig. 3. Equal-area projections of mica (001) (upper row) and chlorite (002) (lower row). Poles to bedding and cleavage are in N–S and E–W directions, respectively. No data can be obtained in the central area of the projections, due to the angular limitation of the transmission mode. Plots are contoured in multiples of random distribution (m.r.d.). Contour interval is 0.3 m.r.d. for all plots. Maximum and first contour for each sample are listed in Table 2.

Table 2. Maximum and first contour for projections in Fig. 3

		Mica		Chlorite	
Sample	Distance	Maximum	Contour (1)	Maximum	Contour (1)
1	6	3.49	0.10	3.60	0.30
2	34	4.80	0.30	4.38	0.10
3	37	3.57	0.20	2.94	0.20
4	50	2.21	0.10	2.58	0.10
5	53	3.04	0.30	2.63	0.20
6	74	3.13	0.10	3.48	0.10
7	77	2.90	0.20	2.30	0.20
8	85	3.03	0.30	4.09	0.10
9	87	2.50	0.10	2.35	0.20
10	91	2.31	0.20	2.27	0.10
11	98	2.43	0.30	2.53	0.10
12	104	2.65	0.20	2.99	0.20
13	128	4.66	0.10	3.77	0.10

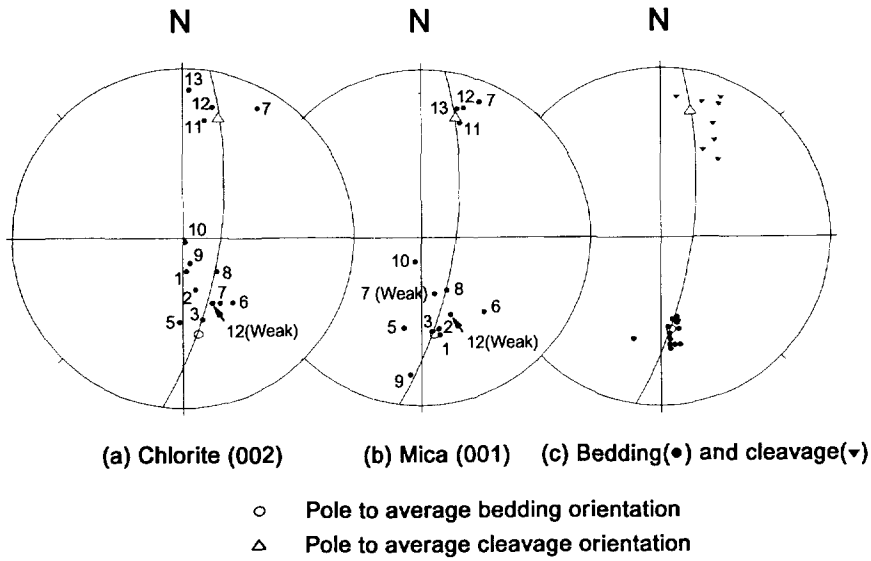

Fig. 4. Equal-area projections of fabric elements in each sample in geographic co-ordinate system; (a) preferred orientation of chlorite (002); (b) preferred orientation of mica (001); and (c) bedding and cleavage orientations. Mean bedding and cleavage orientations are based on measurements across the entire outcrop.

correspond to the areas analyzed with the texture goniometer. It is important to note that such SEM images provide resolution only of phyllosilicate grains 10 μm and larger in longest dimension (2–30 μm in thickness). We refer to these larger grains, rectangular to ovoid or subangular in outline, as detrital, as there is much evidence (see below) to indicate that all or much of the chlorite was originally detrital biotite that was modified during diagenesis and metamorphism (Woodland 1982). On the other hand, grains in the fine-grained matrix, which are presumably largely authigenic in origin, are resolvable only with TEM images.

Samples closer to the contact than sample 6 (Figs. 6a & b) exhibit little deformation, with (001) planes of mica grains being predominantly parallel to bedding and (001) planes of chlorite grains subparallel to bedding. The difference in orientation of chlorite (001) planes and bedding varies with the distance from the contact. In samples 6, 8, 9 and 10 (cf. Figs. 6c–e), deformed mica and chlorite grains have a variety of orientations. In samples beyond sample 11, thin bands of phyllosilicates define the cleavage (Figs. 6f & g). Such bands consist of small grains which are generally too small to be resolved on the SEM scale. However, some small crystals have euhedral shapes, are elongated parallel to cleavage and appear to be authigenic in origin, whereas others appear to be rotated and deformed extensions of grains with detrital shapes that are still largely oriented parallel to bedding.

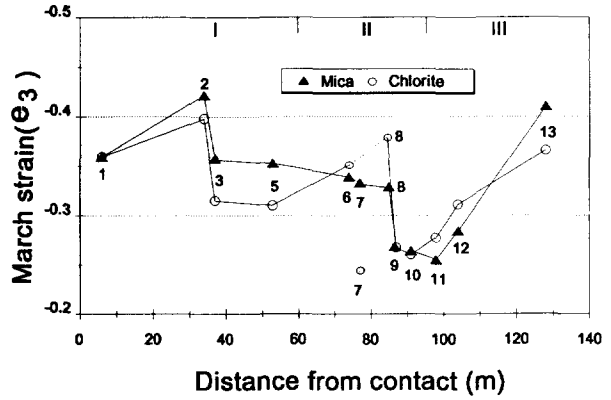

Fig. 5. March strains along the mudstone to slate transition, with samples numbered.

Semi-quantitative energy dispersive spectral (EDS) analyses were performed using a Hitachi S-570 SEM, equipped with a Kevex Quantum EDS system, which is capable of analyzing light elements with atomic number as low as 5 (Boron). Compositions were obtained for mica and chlorite occurring as detrital grains and in the cleavage orientation. Chlorite with detrital-like shapes shows a narrow range of compositions with Mg > Fe, whereas chlorite oriented parallel to cleavage also has a narrow range of compositions, but with Fe > Mg. The composition of detrital mica falls into two well-defined ranges, one having a larger Fe content than the other. Domains with two compositions coexist in detrital grains, as seen by the differences in gray-level contrast in Fig. 6(a). The mica occurring as packets within chlorite-mica stacks has uniformly low Fe content, whereas that in the cleavage is relatively Fe-rich. The data collectively imply that detrital grains, which presumably had a range of compositions, were homogenized during diagenesis to produce chlorite with Mg > Fe and low-Fe mica, the chlorite and mica with larger Fe contents subsequently having formed in the cleavage orientation. These data qualitatively show that mica and chlorite that formed during different events in pelitic rocks may have narrow, characteristic ranges of composition, permitting individual grains to be correlated with individual events.

DISCUSSION

Orientation data are plotted as rakes in a reference plane 098/74 (dip direction/dip) that is perpendicular to the average bedding and cleavage intersection in the

Table 3. March strains of all samples

Sample	Distance	Mica e1	Mica e2	Mica e3	Chl e1	Chl e2	Chl e3
1	6	0.43	0.09	−0.36	0.45	0.08	−0.36
2	34	0.45	0.19	−0.42	0.45	0.15	−0.40
3	37	0.33	0.17	−0.36	0.30	0.13	−0.31
4	50	—	—	—	—	—	—
5	53	0.34	0.15	−0.35	0.29	0.12	−0.31
6	74	0.33	0.14	−0.34	0.32	0.18	−0.36
7	77	0.26	0.17	−0.32	0.18	0.12	−0.24
7	77				0.19	0.11	−0.24
8	85	0.33	0.12	−0.33	0.45	0.12	−0.38
9	87	0.25	0.11	−0.28	0.24	0.10	−0.27
10	91	0.18	0.15	−0.26	0.19	0.13	−0.26
11	98	0.19	0.13	−0.26	0.20	0.15	−0.28
12	104	0.23	0.14	−0.28	0.20	0.20	−0.31
13	128	0.40	0.21	−0.41	0.33	0.18	−0.37

outcrop in order to simplify the presentation, as shown in Fig. 7; the reference plane is also plotted in Fig. 4. The data will be discussed in reference to the three mesoscopic zones recognized in the outcrop.

Mudstone zone

The mudstone zone is characterized by mica and chlorite preferred orientations that are parallel and subparallel to bedding, respectively. Holeywell & Tullis (1975) reported that chlorite has a preferred orientation with a rake approximately 20° less steep than that of mica (which is parallel to bedding), except in those slates where chlorite is parallel to the regional cleavage. However, we observe a trend of convergence of the preferred orientations of chlorite toward mica rather than a constant 20° angular difference with mica and bedding. The preferred orientation of chlorite (002) planes in samples near the contact is up to 30° shallower than bedding, but that value decreases with increasing distance from the contact. At distances further from the contact than sample 5, the preferred orientation of chlorite is parallel to that of mica, and is at a small angle to bedding. This angular difference was further confirmed by SEM observations (Figs. 6a & b) as clearly seen in the large detrital grains.

To account for the angular difference between chlorite and mica preferred orientations in the mudstone, Wintsch (1978) proposed that the chlorite was diagenetic in origin. He hypothesized that whereas the mica inherited an orientation related to a detrital origin, chlorite formed later, following tilting of the beds. However, the SEM images shown here demonstrate that the grains of chlorite resolvable at this scale have a shape typical of detrital grains and are inclined to the mica. Li *et al.* (1994) and others have shown that such chlorite may have originally been some other detrital mineral, biotite being a common precursor, and that the mica packets included within chlorite were introduced after deposition. Nevertheless, even though the chlorite grains have been severely modified, their shapes are typical of detrital grains and most likely reflect depositional conditions. The initial differences in mica and chlorite orientations therefore remain unexplained.

Slate zone

X-ray pole figure data show that both mica and chlorite have preferred orientations in the cleavage direction. SEM images (Figs. 6f & g) clearly show the presence of phyllosilicate-rich bands oriented parallel to cleavage. Qualitative EDS analyses invariably contain contributions from both chlorite and mica, implying that grain sizes are less than the resolution of the method (i.e. < 1 μm), even though the phyllosilicates appear to be homogeneous in SEM images. Large detrital grains exhibit marked strain features, with portions of some grains being bent toward and into the cleavage domains, consistent with mechanical rotation. However, the small crystals of chlorite and mica in the cleavage orientation have Fe-rich compositions characteristic of newly formed phases, which is consistent with neocrystallization from a pore fluid.

Transition zone

Samples 6–10 document the changes in preferred orientations of mica and chlorite from bedding to cleavage orientation. With the exception of sample 7, for which the results are anomalous (both bedding and cleavage fabrics are observed), the pole figure data show that the preferred orientations of both mica (001) planes and chlorite (002) planes progressively trend away from bedding toward the cleavage orientation, starting at about the same position in the outcrop (south of sample 3). This is in contrast to the observation of Holeywell & Tullis (1975) that the chlorite preferred orientation remains parallel to bedding 30 m further along the outcrop than mica. Most importantly, these data demonstrate that, as cleavage develops, there is a gradual, continuous shift in orientation from bedding toward cleavage. Although the maximum shift in orientation is half the difference in cleavage and bedding orientations, it is nevertheless significant in implying that rotation of grains contributes to early cleavage development.

The preferred orientations as indicated by the pole figures for transition zone samples are not as well defined as those in either the mudstone zone or the slate zone. The patterns are more like a band extending across the region between bedding and cleavage orien-

tations. These patterns suggest a distribution of the *c*-axes of mica and chlorite along the plane orthogonal to bedding and cleavage. Moreover, the corresponding decrease in March strains (Fig. 5) further suggests that the *c*-axes are distributed over a wider angular range. These results are also consistent with a significant component of mechanical rotation of phyllosilicate grains.

Holeywell & Tullis (1975) argue that the trend in their pole figure data toward the cleavage orientation may not be caused by mechanical rotation of grains, but that it represents the composite of both cleavage and bedding orientations. However, this is unlikely for two reasons: (1) the pole figure data are able to resolve two separate fabrics, as shown, for example, by sample 7 for which there are two equally intense preferred orientations of chlorite (Fig. 3). Furthermore, a well-defined cleavage orientation and a less well-defined bedding orientation are observed for both mica and chlorite in sample 12 (Fig. 3); (2) SEM images (Figs. 6c–e) clearly show deformed, detrital grains, portions of which are bent toward the cleavage orientation. For example, Fig. 6(c) shows two elongate grains with their ends bent into the cleavage orientation. Such features are commonly observed, and are even better defined for samples in the slate zone. For the latter, phyllosilicates in the slate zone clearly define cleavage, but detrital grains oriented parallel to cleavage and partially rotated into cleavage are common. In addition, detrital phyllosilicates in the transition zone generally appear to be more deformed away from the contact, consistent with the decreasing trend in March strains.

The major difference between samples in the transition and slate zones is the absence of thin phyllosilicate domains oriented approximately parallel to cleavage in the transition zone samples and their presence in slate zone samples. The presence of such grains with no relation to original detrital grains, their unique chemical composition as compared with detrital grains, and the fine intergrowth of chlorite and mica unresolvable by SEM are consistent with formation by dissolution of bedding-parallel grains and neocrystallization in the cleavage orientation. Samples that display this feature, including sample 7, give pole figures indicating a preferred orientation parallel to cleavage. Most importantly, even though pole figures obtained from the transition zone indicate an initial gradual trend toward cleavage, the data indicate that the bulk of the shift toward cleavage occurs over an extremely narrow interval (between samples 10 and 11). This observation provides compelling evidence for dissolution and neocrystallization as an increasingly important mechanism with distance from the contact.

Among the samples in the transition zone, sample 7 is unique because it contains some features like those found in samples of the slate zone. Pole figure data indicate preferred orientation of mica in the cleavage orientation and chlorite in both cleavage and bedding orientations; a corresponding BSE image is shown in Fig. 6(h). We infer that it represents an intermediate stage in cleavage formation in that the change of fabric from bedding to cleavage is complete for mica, but only partially complete for chlorite. Because dissolution and neocrystallization is an important mechanism of cleavage formation, this suggests that the degree of dissolution is measurably different for different minerals.

Our observations in this outcrop collectively show that dissolution and neocrystallization is an important mechanism of cleavage formation, but that there is an important component of mechanical rotation. The latter is contrary to the results of earlier studies. Holeywell & Tullis (1975) showed that mica changes from the bedding orientation to that of cleavage 30 m before there is a corresponding change in the orientation of chlorite. Mechanical rotation would have changed the orientations of both minerals in a similar way, and was therefore rejected in favor of dissolution and neocrystallization. However, Holeywell & Tullis (1975) obtained preferred orientation data by using 'great-circle scans'. Such limited data is in part misleading, as 'maxima' do not always coincide with points along the great circle scan (cf. Fig. 3), which explains the apparent discrepancy with our data.

Lee *et al.* (1986) concluded on the basis of TEM observations that mechanical deformation was virtually absent. Several features were shown as evidence: (1) even at the TEM scale, orientations intermediate to those of bedding and cleavage are absent. (2) The phyllosilicate layers approximately parallel to bedding commonly are terminated against straight layers of grains oriented approximately parallel to cleavage. (3) Strain features were observed only in one instance. However, the data of Lee *et al.* (1986) were obtained only from mineral grains in the fine-grained matrix, whereas direct observations of mechanical rotation are made in SEM images of large detrital grains. It is therefore important to distinguish between the behavior of fine-grained matrix phyllosilicates and large detrital grains. The TEM data are not in conflict with the observations of this paper, in that SEM observations refer only to detrital grains and TEM data were obtained only for authigenic grains, whereas pole figure data reflect orientations of both matrix and detrital components. These relations therefore emphasize the significance of integrated results for minerals occurring at both the TEM and SEM levels of resolution.

CONCLUSIONS

Although dissolution and neocrystallization is the dominant mechanism for cleavage formation observed for matrix phyllosilicates, mechanical rotation of detrital phases plays an important role during the initial stages, as indicated by pole figure data and as shown by SEM. Collectively, these data imply that mechanical rotation and dissolution/neocrystallization are competing mechanisms with the former first being detected at 40 m from the contact based on X-ray data. Within the interval 60–95 m from the contact (transition zone), mechanical rotation dominates the process, as reflected in preferred

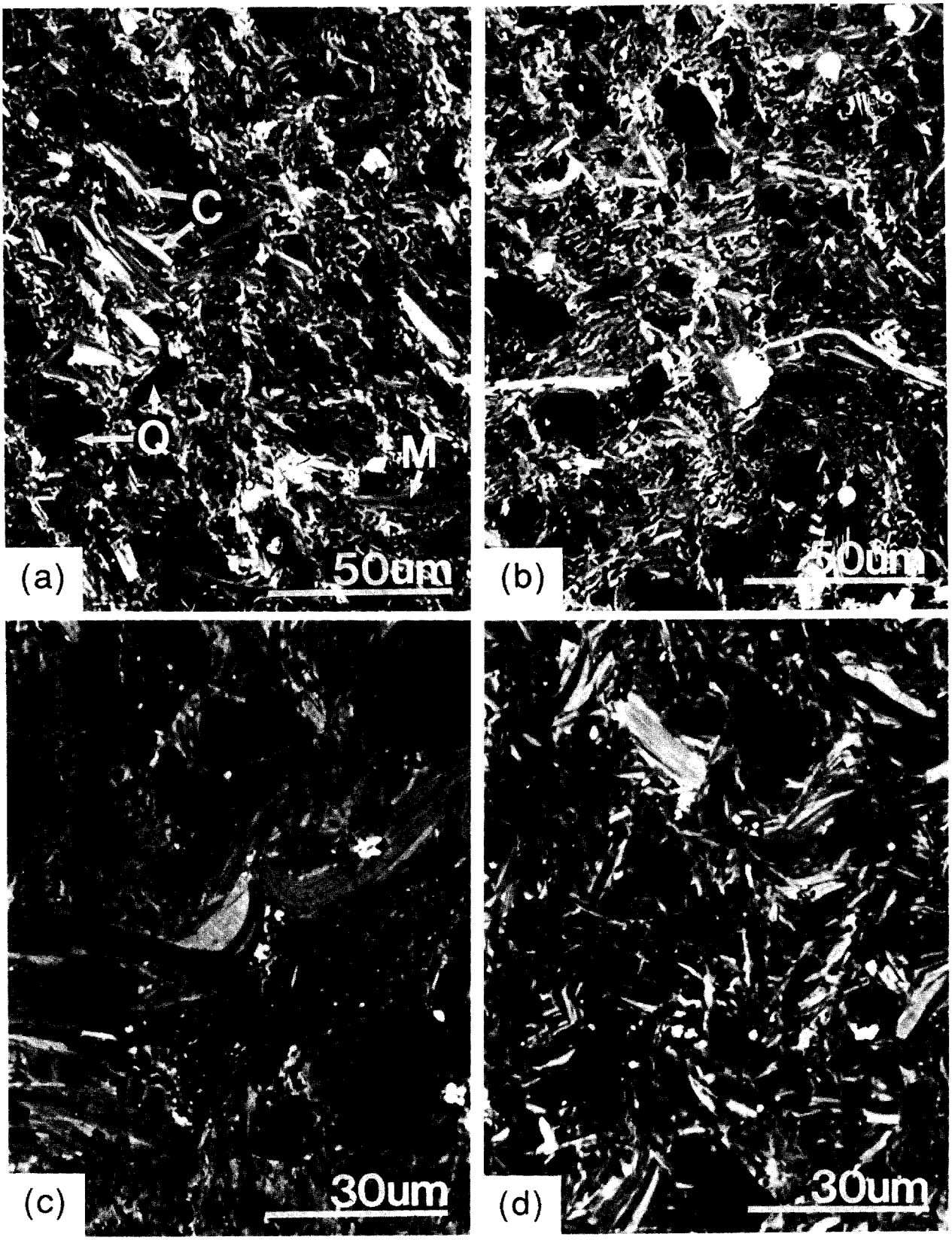

Fig. 6. Selected BSE images of samples: (a) sample 1; (b) sample 5; (c) sample 6; (d) sample 9; (e) sample 10; (f) sample 11; (g) sample 13; (h) sample 7. Mica (M), chlorite (C), and quartz (Q) are labeled in (a); minerals can be identified in the other images as they display the same contrast as in (a).

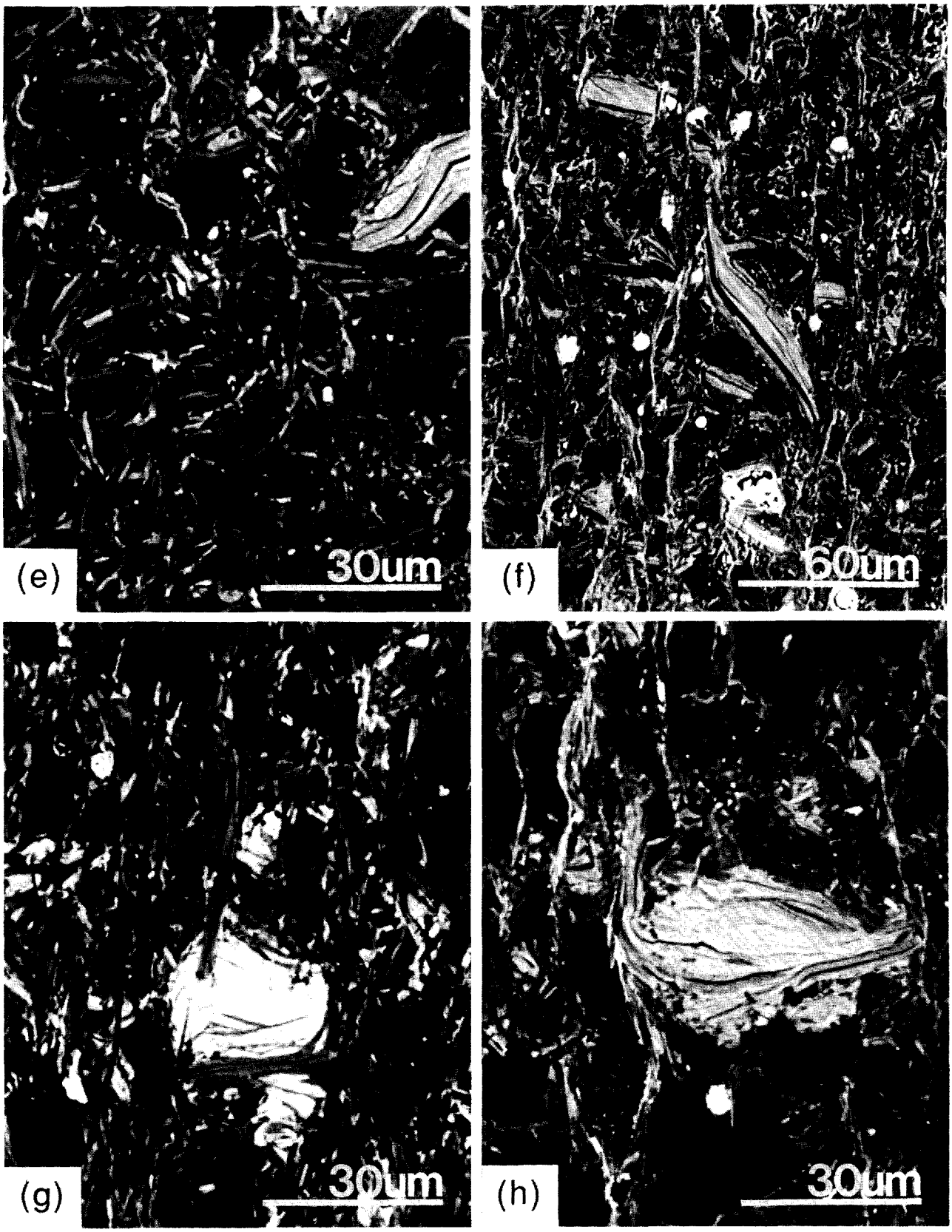

Fig. 6. *Continued*.

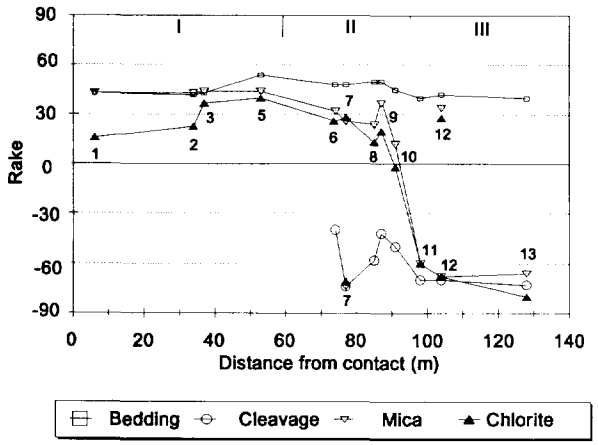

Fig. 7. Orientation of bedding, cleavage, mica (001), and chlorite (002) as a function of the distance from the contact. Bedding and cleavage orientations are based on field measurements; mica and chlorite data are from X-ray preferred orientation measurements. Data are plotted as rakes in the plane 098/74 (dip direction/dip). Three mesoscopic zones are recognized in the outcrop: (I) mudstone zone, (II) transition zone, and (III) slate zone.

orientations that continue to shift toward the cleavage, and a degree of preferred orientation that decreases. Even for the samples from this zone, however, selected portions of detrital grains with orientations parallel to cleavage have Fe-rich compositions indicating that they formed through neocrystallization. In the slate zone, dissolution and neocrystallization was the dominant mechanism, resulting in growth of chlorite and mica in the cleavage orientation, which leads to a well-defined cleavage with high March strains in the fully evolved stages of cleavage formation.

Acknowledgements—The single-crystal diffractometer was acquired under NSF grant EAR-8917350; development of the goniometer stage was supported by NSF grants EAR-9119196 (BvdP) and EAR-9104546 (DRP), the GSA Graduate Student Research Fund and the Scott Turner Fund (NCH). Data were obtained with the support of the American Chemical Society-Petroleum Research Fund (grant 27461-AC8). We are grateful to E. Erslev, P. Hudleston, and R. Wintsch for thorough reviews and constructive comments on the paper. B. A. Housen is thanked for providing samples and discussion. Special thanks are due to G. Oertel (UCLA), and H.-R. Wenk (UC Berkeley), who generously shared their time and expertise, and made valuable suggestions about the technical aspects of pole figure analysis. Contouring programs were provided by H.-R. Wenk.

REFERENCES

Alterman, I. B. 1973. Rotation and dewatering during slaty cleavage formation: some new evidence and interpretations. *Geology* **1**, 33–36.

Beutner, E. C. 1978. Slaty cleavage and related strain in Martinsburg slate, Delaware Water Gap, New Jersey. *Am. J. Sci.* **278**, 1–33.

Boulter, C. A. 1974. Tectonic deformation of soft sedimentary clastic dikes from the Precambrian rocks of Tasmania, Australia, with particular reference to their relations with cleavage. *Bull. geol. Soc. Am.* **85**, 1413–1420.

Carson, W. P. 1968. Development of flow cleavage in the Martinsburg shale, Port Jervis South area (northern New Jersey). *Tectonophysics* **5**, 531–541.

Chen, R. T. & Oertel, G. 1989. Strain history of the Los Prietos syncline, Santa Maria basin, California: a case of post-tectonic compaction. *J. Struct. Geol.* **11**, 539–551.

Chen, R. T. & Oertel, G. 1991. Determination of March strain from phyllosilicate preferred orientation: a semi-numerical method. *Tectonophysics* **200**, 173–185.

Engelder, T. & Marshak, S. 1985. Disjunctive cleavage formed at shallow depths in sedimentary rock. *J. Struct. Geol.* **7**, 327–343.

Epstein, J. B. & Epstein, A. G. 1969. Geology of the Valley and Ridge province between Delaware Water Gap and Lehigh Gap, Pennsylvania. In: *Geology of Selected Areas in New Jersey and Eastern Pennsylvania and Guidebook of Excursion, New Brunswick, New Jersey* (edited by Subitzky, S.). Rutgers University Press, 132–205.

Etheridge, M. A. & Oertel, G. 1979. Strain measurements from phyllosilicate preferred orientation—a precautionary note. *Tectonophysics* **60**, 107–120.

Hobbs, B. E., Means, W. D. & Williams, P. F. 1976. *An Outline of Structural Geology*. John Wiley & Sons Inc., New York.

Holeywell, R. C. & Tullis, T. E. 1975. Mineral reorientation and slaty cleavage in the Martinsburg Formation, Lehigh Gap, Pennsylvania. *Bull. geol. Soc. Am.* **8**, 1296–1304.

Housen, B. A. & van der Pluijm, B. A. 1991. Slaty cleavage development and magnetic anisotropy fabrics. *J. geophys. Res.* **96** (B6), 9937–9946.

Housen, B. A., van der Pluijm, B. A. & Van der Voo, R. 1993. Magnetite dissolution and neocrystallization during cleavage formation: paleomagnetic study of the Martinsburg Formation, Lehigh Gap, Pennsylvania. *J. geophys. Res.* **98**, 13,799–13,813.

Kamb, W. B. 1959. Theory of preferred orientation developed by crystallization under stress. *J. Geol.* **67**, 153–170.

Keith, A. 1894. Harpers Ferry, Va.-W. Va.-Md. U.S. Geological Survey Geological Atlas, Folio 10.

Lash, G. G. 1987. Sedimentology and possible paleoceanographic significance of mudstone turbidites and associated deposits of the Pen Argyl member, Martinsburg Formation (upper Ordovician), eastern Pennsylvania. *Sediment. Geol.* **54**, 113–135.

Lee, J. H., Peacor, D. R., Lewis, D. D. & Wintsch, R. P. 1986. Evidence for syntectonic crystallization for the mudstone to slate transition, at Lehigh Gap, Pennsylvania, U.S.A. *J. Struct. Geol.* **8**, 767–780.

Li, G., Peacor, D. R., Merriman, R. J., Roberts, B. & van der Pluijm, B. A. 1994. TEM and AEM constraints on the origin and significance of chlorite–mica stacks in slates: an example from Central Wales, U.K. *J. Struct. Geol.* **16** (8), 1139–1157.

March, A. 1932. Mathematicsche Theorie der Regelungen nach der Korngestalt bei affiner deformation. *Z. Kristallogr. Mineral. Petrogr.* **1**, 258–297.

Maxwell, J. C. 1962. Origin of slaty and fracture cleavage in the Delaware Water Gap area, New Jersey and Pennsylvania. In: *Mem. geol. Soc. Am. (Buddington Volume)*: New York, 281–311.

Oertel, G. 1970. Deformation of a slaty, lapillar tuff in the Lake District, England. *Bull. geol. Soc. Am.* **81**, 1173–1188.

Oertel, G. 1983. The relationship of strain and preferred orientation of phyllosilicate grains in rocks—a review. *Tectonophysics* **100**, 413–447.

Schulz, L. G. 1949. A direct method for determining preferred orientation of a flat reflection sample using a Geiger counter X-ray spectrometer. *J. Appl. Phys.* **20**, 1033–1036.

Sorby, H. C. 1853. On the origin of slaty cleavage. *Edinburgh New Phil. J.* **55**, 137–148.

Stephens, G. C. & Wright, T. O. 1981. Stratigraphy of the Martinsburg formation, west of Harrisburg in the Great Valley of Pennsylvania. *Am. J. Sci.* **281**, 1009–1020.

Tullis, T. E. & Wood, D. S. 1975. Correlation of finite strain from both reduction bodies and preferred orientation of mica in slate from Wales. *Bull. geol. Soc. Am.* **86**, 632–638.

van der Pluijm, B. A. & Kaars-Sijpesteijn, B. H. 1984. Chlorite–mica aggregates: Morphology, orientation, development and bearing on cleavage formation in very low-grade rocks. *J. Struct. Geol.* **6**, 399–407.

van der Pluijm, B. A., Ho, N.-C. & Peacor, D. R. 1994. High-resolution X-ray texture goniometry. *J. Struct. Geol.* **16** (7), 1029–1032.

Wenk, H-.R. 1985. *Preferred Orientation in Deformed Metal and Rocks: An Introduction to Modern Texture Analysis*. Academic Press Inc., Orlando.

White, S. H. & Knipe, R. J. 1978. Microstructure and cleavage development in selected slates. *Contr. Miner. Petrol.* **66**, 165–174.

Williams, P. F. 1972. Development of metamorphic layering and cleavage in low-grade metamorphic rocks at Bermagui, Australia. *Am. J. Sci.* **272**, 1–47.

Wintsch, R. P. 1978. A chemical approach to the preferred orientation of mica. *Bull. geol. Soc. Am.* **89**, 1715–1718.

Wintsch, R. P. 1985. The possible effects of deformation on chemical

processes in metamorphic fault zones. In: *Metamorphic Reactions: Kinetics, Textures, and Deformation* (edited by Thompson, A. H. & Rubie, D. C.). Springer-Verlag Inc., New York, 251–268.

Wintsch, R. P., Kvale, C. M. & Kisch, H. J. 1991. Open-system, constant-volume development of slaty cleavage, and strain-induced replacement reactions in the Martinsburg Formation, Lehigh Gap, Pennsylvania. *Bull. geol. Soc. Am.* **103**, 916–927.

Wintsch, R. P. & Kunk, M. J. 1992. $^{40}Ar/^{39}Ar$ evidence for Alleghanian age of the slaty cleavage in the Martinsburg Formation, Lehigh Gap area, Pennsylvania. *Geol. Soc. Am. Abs. w. Prog.* **24**, 85.

Wood, D. S. 1974. Current views on the development of slaty cleavage. *Annu. Rev. Earth & Planet. Sci.* **2**, 369–401.

Woodland, B. G. 1982. Gradational development of domainal slaty cleavage, its origin and relation to chlorite porphyroblasts in the Martinsburg Formation, eastern Pennsylvania. *Tectonophysics* **82**, 89–124.